Publ. Astron. Obs. Belgrade No. 64 (1999), 103 - 111 *Invited paper*

NEW NARROW AND BROAD BAND IMAGES OF THE RINGED SEYFERT 2 GALAXY MARK 620

I. YANKULOVA
Department of Astronomy, Faculty of Physics,
St Kl. Okhridski University of Sofia, 5 James Bourchier St,
BG - 1126 Sofia, Bulgaria
E-mail YAN@PHYS.UNI-SOFIA.BG.

Abstract. We present new flux calibrated narrow and broad band images of the circumnuclear region of Seyfert 2 galaxy Mark 620 = NGC 2273 in the light of [O III] λ4959 Å , [O I] λ6364 + [Fe X] λ 6374 Å Å and [N II] λ6548 Å emission lines and two continuum images at λ6300 Å and λ 4260 Å , and in broad band *Gunn r* continuum.

The color map $F_\lambda(6300\text{Å})/F_\lambda(4260\text{Å})$ reveals a dusty ringlike structure around the nucleus of Mark 620.

Based on the color map $F_\lambda(6300\text{Å})/F_\lambda(4260\text{Å})$ we have estimated an extinction of $A_V = 1^m\!.04$ which yields $10^5 \times M_\odot$ for the mass of the dust in the ring.

1. Introduction

In recent years, several arguments have been advanced to indicate that galaxy interactions and/or orbital resonances can lead to the enhanced fueling of various kinds of nuclear activity, especially the Seyfert and Starburst phenomena (Heckman 1990, 1991; Dultzin-Hacyan, 1997).

In the theory of AGNs the luminous ($L_{IR} > 10^{10} L_\odot$) IRAS galaxies play an important role. Studies of dust and gas distribution in the circumnuclear regions of luminous IRAS AGNs galaxies with rings and bars provide an information both about the link between the AGN and star formation events and about the matter transport to the active nucleus.

NGC 2273 (Mark 620) was discovered by Huchra et al.(1982) to be a type 2 Seyfert galaxy and classified by de Vaucouleurs et al., 1991 [RC3] as a morfological type SB(r)a:. The heliocentric recession velocity is $cz = 1875$ km sec^{-1} [RC3].

NGC 2273 has been detected by IRAS (Lonsdale, Lonsdale & Smith, 1992 hereafter LLS92) with strong far infrared emission (FIR) $L_{FIR} \sim 10^{10} L_\odot$.

The continuum measurements by Krugel et al. (1988) at 1300 μm and the spectral index between 100 and 1300 μm clearly indicate that the emission must be thermal reradiation from dust.

The mid-infrared emission of Mark 620 at 10 μm measured by Devereux (1987) in small aperture ($\sim$5 arcsec) is due to thermal dust reradiation of the UV/optical emission of the central source (Giuricin et al.,1995).

CCD interference-band images isolating the emission lines of Hα + [N II] and [O III] λ5007 were obtained by Pogge (1989) and Mulchaey, Wilson and Tsvetanov (1996) (hereafter MWT96) to search for spatially extended circumnuclear emission regions.

We present the results of new narrow and broad-band imaging to study gas and dust distribution in the circumnuclear region of the ringed Seyfert 2 galaxy Mark 620.

2. Observations and data reduction

2. 1. OBSERVATIONS

Mark 620 has been observed with the 2m Ritchey-Chretien-Coudé (2-m RCC) reflector of the Bulgarian National Astronomical Observatory (BNAO) at Mount St. Spirit near Rozhen, Rodopa mountains. The observations were carried out on December 12, 1992.

The narrow-band images were taken with the Focal Reducer of the Max-Planck-Institute for Aeronomy (MPAe). The technical data and the capabilities of the MPAe Focal Reducer are described by Jockers (1992).

The telescope/reducer configuration and the CCD's square 22 μm pixels provide an image scale of $0''.8$ px^{-1}.

Images through interference filters centered near the wavelengths of [N II] λ6548 [O III] λ4959 and [O I] λ6364 + [Fe X] λ 6374 ("on-line") and on the emission free continuum windows at λ4260 and λ6300 ("off-line") were obtained. The "off-line" images were used to subtruct the continuum contribution contained in the "on-line" images. Moreover, the "off-line" images were used to form the color map.

A broad band image was obtained with *Gunn r* interference filter.

Table 1. M 620 - observing log and related data.

image frame	interference filter, $\lambda_c/\Delta\lambda$ (Å)/(Å)	exposure time (s)	final FWHM resolution (arcsec)
[N II] λ6548	6567/30	1×300	4.4
[O I] λ6364 + [Fe X] λ 6374	6420/30	2×300	3.2
red continuum	6300/34	2×300	3.2
[O III] λ4959	5003/40	2×300	2.7
blue continuum	4260/34	2×300	3.1
Gunn r	6550 /900	2×300	4.3

The observing log is presented in Table 1 where the central wavelengths λ_c and the effective width $\Delta\lambda$ of the interference filters, and the spatial resolution of the images in terms of the point-spread function (PSF) are listed.

2. 2. DATA REDUCTION

The images were reduced following the usual reduction steps for narrow-band imaging (Haniff, Wilson & Ward 1988 ; Perez-Fournon & Wilson 1990 ; Tsvetanov & Walsh 1992).

After flat-fielding the frames were aligned by rebinning to a common origin. The final alignment of all the images was estimated to be better than 0.″1. As an unwanted by-product of the rebinning procedure a small decrease of the resolution (~ 0.″15) was noticeable. The two images taken through the same filter were averaged and the cosmic-ray signatures were removed.

Unfortunately, small tracking errors of the 2-m RCC telescope caused residual ellipticities in the PSFs of our frames. Therefore, a convolution procedure was performed in order to match the PSFs of each line – continuum pair. The same procedure has been applied to those images which later were used in the mapping of continuum emission ratios. This degraded the final resolution to a mean value of ~3.″3.

3. Results

3. 1. BROAD AND NARROW - BAND CONTINUUM IMAGES

Contour map of the broad band r continuum is presented in Fig.1. Several morphological features are clearly seen : the outermost pseudoring structure at radius of 7.3 kpc (≈ 60 arcsec); an ovally distorted disk with a radius of about 30 arcsec. The innermost visible structure is a bar with P.A.≈ 114° . Weak spiral arms originate from the bar and form an inner pseudoring with radius ≈ 2.4 kpc (≈ 20 arcsec). Similar features have been noted and discussed by Gallagher & Wirth (1980) and van Driel & Buta (1991).

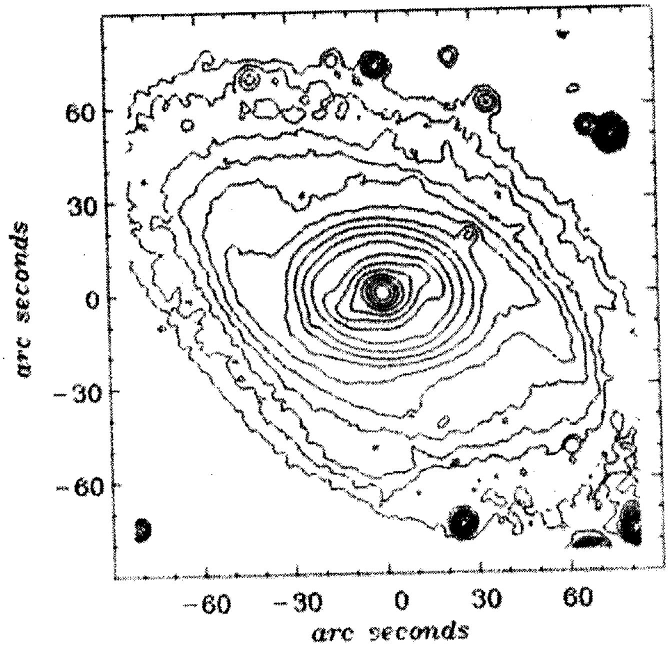

Fig. 1. CCD *Gunn r* contour plot. First contour is at 2σ from the background (1σ background noise level is 3×10^{-18} ergs cm^{-2} s^{-1}arcsec^{-2}Å^{-1}). The other contours increase as a power series of 2.

It should be noted, the *Gunn r* continuum contour map (Fig.1) shows an isophotal twist in the innermost region of Mark 620. Similar isophotal twists are observed in early type spirals and could be associated with inner Lindblad resonances (ILR) (Elmegreen et al.,1996).

The continua images obtained at $\lambda\,4260$ Å and $\lambda\,6300$ Å were used to create the narrow-band color map, presented in Fig. 2, where "black" means excess of light while "white" means absorption.

The color map (Fig. 2) reveals an inner redder structure reminding of dusty ring around the AGN nucleus of Mark 620. This ringlike structure has a diameter of about 14 arcsec corresponding to $\approx$ 1700 pc. Its mean projected thickness is about 500 pc.

A second dusty ring is clearly seen on the color map. Its radius is $\approx$ 20 arcsec (2.4 kpc) and is approximately placed on the inward side of the ovally distorted disk. Gallagher & Wirth (1980) have also shown the presence of outer rather red ring.

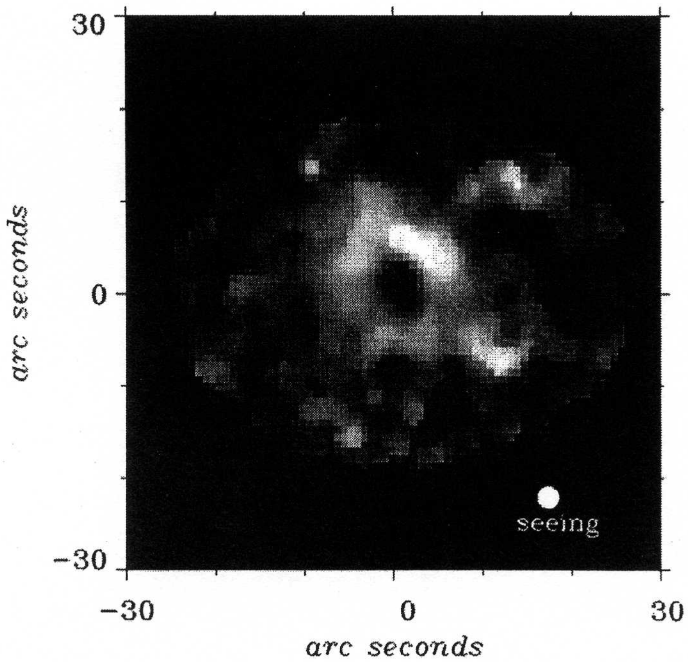

Fig. 2. Red/blue narrow-band color map of Mark 620.

3. 2. NARROW - BAND EMISSION LINE IMAGES

The emission line contours of [O III] λ4959 and [N II] λ6548 , [O I] λ6364 + [Fe X] λ 6374 superimposed on the F_λ(6300Å)/ F_λ(4260Å) color map are presented in Fig.3 and Fig.4.

The corresponding $1\,\sigma$ background noise levels in the emission line images are presented in Table 2. The lowest isophotal level is at $3\,\sigma$ above the sky subtraction level and the following contours are multiplied with $\sqrt{2}$.

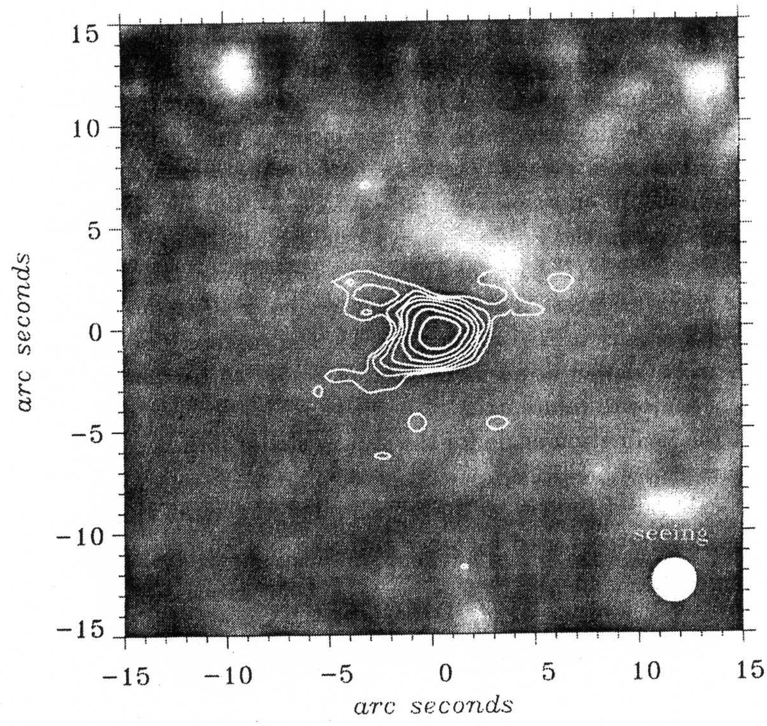

Fig. 3. The [O III]λ4959 Å -emission contours superimposed over the red/blue narrow-band color map.

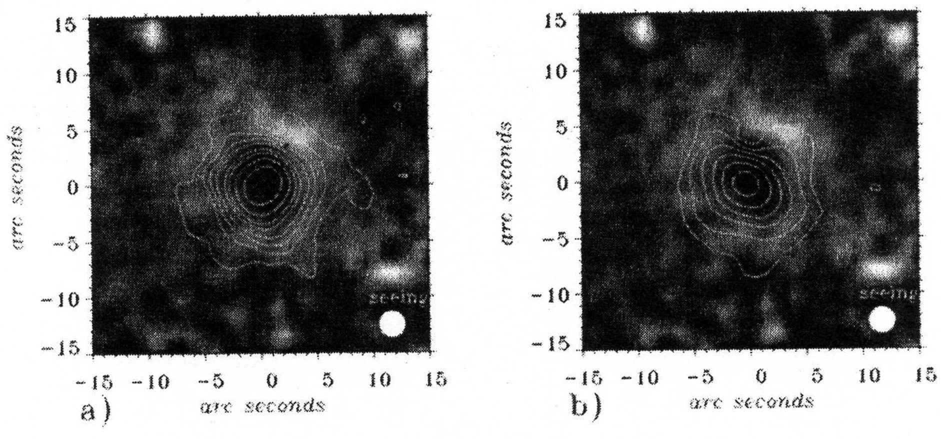

Fig. 4. a) The [N II]λ6548 Å -emission contours superimposed over the red/blue narrow-band color map, b) [OI]λ6364 + [FeX]λ6374 Å Å over the same map.

The [O III] λ4959 emission arises entirely in the circumnuclear region enclosed by the dusty ring and is strongly reduced where the dust content is enhanced.

The emission [N II] λ6548 Å (Fig.4a) shows extended emission in diameter of about 18 arcsec. The image morphology does not differ from that of the Hα + [N II] $\lambda\lambda$ 6548/84 Å Å image presented by MWT96. The outermost contour in Fig.4a, which is at 3 σ above the noise level, entirely includes the dusty ring.

The [O I] emission is a good diagnostic tool for the presence of hard nonthermal ionizing photons. Both emission lines [O I] λ6364 Å and [Fe X] λ 6374 Å (Fig.4b) are transmited through the F 642.

The *Gunn r* contours (Fig.1), the color map (Fig.2) and the presence of extended emission line regions suggest that the ionized region is a gaseous disk with an orientation of the major axis at P.A. $\approx$ 20° (Fig. 1). The gaseous disk wound by the dusty ring appears to be viewed at an inclination of $\sim$ 32° to the line of sight, estimated by the ratio of major to minor axes.

Note that the inclination angle for the galaxy stellar disk is $\sim$ 45° (Whittle 1992; de Vaucouleurs et al.1991 [RC3]).

From our calibrated images we have estimated the total fluxes of the observed emission lines in apertures used by other authors.

4. DISCUSSION

4. 1. GAS AND DUST IN THE NARROW LINE REGION IN MARK 620

Previous studies of Mark 620 have revealed a strong [O III] λ5007 Å emission concentrated around the nucleus and circumnuclear extended emission of Hα + [N II] $\lambda\lambda$ 6548/84 Å Å (Pogge, 1989; MWT96).

The colour map $F_\lambda(6300\text{Å})/F_\lambda(4260\text{Å})$ (Fig.2) infers the presence of a redder dusty ringlike structure around the AGN nucleus of Mark 620. Otherwise, the innermost circumnuclear region is not influenced by extinction. We assume that the circumnuclear emission line region with diameter of about 700 - 800 pc, where the [O III] λ4959 Å contours are situated, is a high ionized Strömgren zone (Fig.3) . The Strömgren depth is defined as

$$N^S_{H+} = c\,\Gamma/\alpha_B \approx 10^{23}\,\Gamma \quad \text{cm}^{-2},$$

where α_B cm^3 sec^{-1} is the recombination coefficient to excited states of hydrogen, c is the speed of light and Γ is the ionization parameter. In order to estimate Γ we take the electron density $\approx$ 600 cm^{-3} following LLS92. The nonthermal component of the ionizing continuum $F_\nu \approx \nu^{-\alpha}$ amounts 0.74 of the measured flux, F_λ(4260Å). Taking a resonable value for $\alpha \approx 1.5$ we estimate the ionizing parameter $\Gamma \approx 10^{-3}$ which yields $N^S_{H+} \approx 3.0 \times 10^{20}$ cm^{-2}.

The [N II] λ6548 Å image (Fig.4a) and the Hα + [N II] image presented by MWT96 show that the Hα + [N II] emission arises both in the inner Strömgren zone and in the dusty ring. Thus the redder dusty ringlike structure appears to be a large partially ionized zone (hereafter *PIZ*) in which the ionized gas becomes neutral. The existence of this large *PIZ* results from harder photons of the ionizing continuum .

In our color map (Fig.2 and see also Fig.3) the Strömgren zone appears to be homogenous and we assume that the measured flux ratio $F_{\lambda\,6300}/F_{\lambda\,4260} = 1.5$ is not reddened there. But in the *PIZ*, where the dust content is enhanced this ratio is influenced by dust extinction (absorption and scattering) and it is about 2.5 . The dust opacity τ_λ^{dust} is given by

$$\tau_\lambda^{dust} = \mu\, N_{H^0}(PIZ)\,(\sigma/H),$$

where σ/H (cm^2 per hydrogen nucleus) is the total extinction cross section and μ is the dust content of the medium expressed relative to the standart *ISM* dust-to-gas mass ratio (Binette et al. 1993). We assume $\mu = 1.0$ and take σ/H from Drain & Lee (1984) (see their Fig. 7) . Based on the reddened and unreddened flux ratios $F_{\lambda 6300}/F_{\lambda 4260}$ we have estimated the column density in the $PIZ\ N_{H^0}(PIZ) \approx 2.0\times 10^{21}$ cm^{-2}. Then the total column density is

$$N_H^{slab} = N_{H^+}^S + N_{H^0}(PIZ) \approx 2.3 \times 10^{21}\mathrm{cm}^{-2}.$$

The column density N_H^{slab} defines the depth of the complete "photoexcited" region, that is the depth at which the incoming ionizing flux is exhausted.

The extinction opacity at 5500 Å is $\tau_V = 4.8 \times 10^{-22}\,\mu\, N_{H^0}(PIZ) = 0.96$ and the extinction is $A_V = 1.086\tau_V = 1^m\!.04$ if $\mu = 1.0$. Following Spitzer (1978) we can estimate the mean dust density along the line of sight $\rho_{\rm dust}$:

$$\rho_{\rm dust} = 1.3\,10^{-27}\rho_s < A_V/L_{kpc} > \left(\frac{\epsilon_o + 2}{\epsilon_o - 1}\right), \mathrm{gcm}^{-3}$$

where ρ_s is the density of the particular dust grains and we assume $\rho_s \approx 1.0$ g cm^{-3}. The dielectric dust function ϵ_o in the low frequency's limit is $\epsilon_o \approx 4$ (Spitzer 1978). The mean extent of the dusty ringlike structure measured on the color map is $L_{kpc} = 0.5\,kpc$. Thus we obtain the mean dust density along the line of sight $\rho_{\rm dust} = 7 \times 10^{-27}$ g cm^{-3}.

From Fig.2 we can roughly estimate the volume occupied by the dusty ring $\approx 4\times 10^{64}$ cm^3, assuming a filling factor of $\approx$ 1. Knowing $\rho_{\rm dust}$ we found that the dust mass contained by the observed dusty ring is $M_{ring} \approx 1.5 \times 10^5$ M$_\odot$. This value is an upper limit since a filling factor of $\approx$ 1 has been assumed.

Balmer decrement.

The Balmer emission lines could be affected by the presence of *PIZ* in the circumnuclear region of Mark 620. The measured Balmer decrement by LLS92 in Mark 620 is $(H_\alpha/H_\beta)_{obs} \approx 7$. After a correction for the reddening we obtain a dereddened Balmer decrement $\approx$ 4.9.

Binette et al.,(1993) show the integrated Balmer lines of a power-law photoionized gas in a system of clouds with internal dust would be significantly affected because of dust and perspective. The same authors argue the intrinsic Balmer decrement could be as steep as 4 - 4.4 in the radiation bounded case where many clouds are seen from the back side.

Dust ringlike morphologies

Dust ringlike morphologies in Seyfert galaxies could be traced both by red / blue color maps and by mid - infrared radiation. The 10.8 μm maps of the central region of the infrared - luminous barred galaxies NGC 1068 and NGC 1097 show the morphologies like kiloparsec - size rings which are intimately associated with the dense neutral interstellar gas inferred from *CO* maps (Telesco, Dressel and Wolstencroft, 1993).

Moreover, in these two galaxies the observed dust ringlike morphologies coincide with the ILRs and demonstrate the role played by bars and oval distortions in the genesis of starbursts (Telesco, Dressel and Wolstencroft, 1993).

If there are extended dusty clouds around Seyfert nuclei, they would show excess emission at *FIR* because the equilibrium temperature is about 100 K (Granato, Danese, & Francheschini 1996; Taniguchi et al.1997). In many objects, these dusty clouds are also connected with the occurrence of the circumnuclear starburst regions. Their typical radii range from several 100 pc to 1 kpc (Telesco et al. 1984; Boer & Schulz 1993; Genzel et al. 1995; Storchi-Bergmann et al. 1996). Arguments favoring the enhanced star formation around the nuclei of Seyfert galaxies as an alternative of the Unified model are presented by Dultzin-Hacyan (1995).

On the other hand, the accumulation of large amount of gas and dust near the ILR is connected with the supply of gas to the nucleus of Seyfert galaxies. Wada and Habe (1992;1995) have found a new fuelling mechanism from kpc to several tens of pc, which is induced by a weak bar and the self-gravity of the gas in a massive gaseous disc. In their model the first ILR is essential for gas accumulation near the centre. The second ILR occupies, roughly, a dimeter of about $\sim 1 - 2$ kpc.

The dust ringlike structure ($\sim$ 1700 pc in diameter (Fig.2)) observed in Mark 620 could be associated with a shocked dust connected with the ILRs.

As a rule, the dust ringlike morphologies favore type 2 Seyfert galaxies which possess SB morphology.

Acknowledgements

I would like to thank Prof. Klaus Jockers, Max-Planck-Institut für Aeronomie, Germany, for kindly providing the focal reducer, interference filters and CCD-camera for use at the 2m telescope of BNAO, and for numerous fruitful discussions about the effective use of this instrumentation. This collaboration was partially supported by the Deutsche Forschungsgemeinschaft, Aktenzeichen 436 BUL 113/61.

I am grateful to Tanyu Bonev, Institute of Astronomy, Bulgarian Academy of Sciences and to Valeri Golev, St.Kliment Okhridski University of Sofia who provided helpful discussions.

I would like to thank Zlatan Tsvetanov, Johns Hopkins University, who provided helpful discussions and comments.

The images were partly processed on a DECpc 450 D_2LP, granted by the European Southern Observatory in the framework of it's Central & Eastern Europe Programme, project number A-03-031.

Our research was supported by the Bulgarian National Scientific Foundation grant under contracts No. F-482/1995 and No. F-484/1995 with the Bulgarian Ministry of Education and Sciences.

This research has made use of the NASA/IPAC Extragalactic Database (NED) which is operated by the Jet Propulsion Laboratory, California Institute of Technology, under contract with the National Aeronautics and Space Administration.

References

Binette, L., Wang, J., Villar-Martin, M., Martin, P.G. and Gladis Magris, C.: 1993, *Astrophys. J.*, **414**, 535.

Boer, B., Schulz, H.: 1993, *Astron. Astrophys.*, **277**, 397.

de Vaucouleurs, G., et al.: 1991, 3rd Reference Catalogue of Bright Galaxies, New York: Springer-Verlag (RC3).

Devereux, N.A.: 1987, *Astrophys. J..*, **323**, 91.

Draine, B.T. and Lee, H.M.: 1984, *Astrophys. J.*, **285**, 89.

Dultzin-Hacyan, D.: 1997, *Rev. Mex. Astron. and Astrof.* SC 6.

Dultzin-Hacyan, D.: 1995, *Rev. Mex. Astron. and Astrof.* SC 3, 31 - 37.

Elmegreen, D.M. and Elmegrren, B.G.: 1996, to be published in the *Astronomical Journal*, June 1996.

Gallagher, J.S. and Wirth, A.: 1980, *Astrophys. J.*, **241**, 567.

Genzel, R. et al.: 1995, *Astrophys. J.*, **444**, 129.

Giuricin, G., Mardirossian, F. and Mezzetti, M.: 1995, *Astrophys. J.*, **446**, 550.

Granato, G.L., Danese, L. and Francheschini, A.: 1996, *Astrophys. J.*, **460**, L11.

Haniff, C.A., Wilson, A.S. and Ward, M.J.: 1988, *Astrophys. J.*, **334**, 104.

Huchra, J.P., Wyatt, W.F. and Davis: 1982, *Astron. J.*, **87**, 1628.

Heckman, T.: 1990, IAU Colloquium 124, Paired and Interacting Galaxies, eds. J.W. Sulentic, W.C. Keel and C.M. Telesco (NASA Conf.Publication 3098), p.359.

Heckman, T.: 1991, in Proc. Conf. Massive Stars in Starbursts, eds. N.R. Leitherer, T.M. Walborn, C.A. Heckman, C.A. Norman (Cambridge: Cambridge University Press), 289.

Jockers, K.: 1992, *Astronomische Gesellschaft Abstr. Ser.* No.7, P108, 184.

Krugel, E., Chini, R., Kreysa, E. and Sherwood, W.A.: 1988, *Astron. Aph.*, **190**, 47.

Lonsdale, C.J., Lonsdale, C.J. and Smith, H.E.: 1992, *Astrophys. J.*, **391**, 629 (LLS92).

Mulchaey, J.S., Wilson, A.S., Tsvetanov, Z.: 1996, *ApJS*, **102**, 309 (MWT96).

Perez-Fournon, L. and Wilson, A.S.: 1990, *Astrophys. J.*, **356**, 456.

Pogge, R.W.: 1989, *Astrophys. J.*, **345**, 730.

Spitzer, L.Jr.: 1978, Physical Processes in the Interstellar Medium, Princeton University Observatory.

Storci-Bergmann, T., Rodriguez-Ardila, A., Schnidt, H.R., Wilson, A.S. and Baldwin, J.P.: 1996, *Astrophys. J.*, **472**, 83.

Taniguchi, Y., Sato, Y., Kawara, K., Murayama, T. and Mouri, H.: 1997, *Astron. Astrophys.*, **318**, L1.

Tsvetanov, Z. and Walsh, J.R.: 1992, *Astrophys. J.*, **386**, 485.

Telesco, C.M., Beclin, E.E., Wynn-Williams, C.G. and Harper, H.D.A.: 1984, *Astrophys. J.*, **282**, 427.

Telesco, C.M., Dressel, L.L. and Wolstencroft, R.D.: 1993, *Astrophys. J.*, **414**, 120.

van Driel, W. and Buta, R.J.: 1991, *Astron. Astrophys.*, **245**, 7.

Wada, K. and Habe, A.: 1992, *Monthly Notices Roy. Astron. Soc.*, **258**, 82.

Wada, K. and Habe, A.: 1995, *Monthly Notices Roy. Astron. Soc.*, **277**, 433.

Whittle, M.: 1992, *ApJS*, **79**, 49.